HOKKAIDO UNIVERSITY

Title	Involvement of SLC16A1/MCT1 and SLC16A3/MCT4 in l-lactate transport in the hepatocellular carcinoma cell line
Author(s)	Mukai, Yuto; Yamaguchi, Atsushi; Sakuma, Tomoya et al.
Citation	Biopharmaceutics & drug disposition, 43(5), 183-191 https://doi.org/10.1002/bdd.2329
Issue Date	2022-09-14
Doc URL	https://hdl.handle.net/2115/90650
Rights	This is the peer reviewed version of the following article: https://onlinelibrary.wiley.com/doi/full/10.1002/bdd.2329, which has been published in final form at https://doi.org/10.1002/bdd.2329. This article may be used for non-commercial purposes in accordance with Wiley Terms and Conditions for Use of Self-Archived Versions. This article may not be enhanced, enriched or otherwise transformed into a derivative work, without express permission from Wiley or by statutory rights under applicable legislation. Copyright notices must not be removed, obscured or modified. The article must be linked to Wiley's version of record on Wiley Online Library and any embedding, framing or otherwise making available the article or pages thereof by third parties from platforms, services and websites other than Wiley Online Library must be prohibited.
Type	journal article
File Information	BDD Mukai et al Manuscript com.pdf

Hokkaido University Collection of Scholarly and Academic Papers : HUSCAP

Title

Involvement of *SLC16A1*/MCT1 and *SLC16A3*/MCT4 in L-lactate transport in the hepatocellular carcinoma cell line

Abstract

Fourteen isoforms of the monocarboxylate transporter (MCT) have been reported. Among the MCT isoforms, MCT1, MCT2, and MCT4 play a role in L-lactate/proton co-transport and are involved in the balance of intracellular energy and pH. Therefore, MCT1, MCT2, and MCT4 are associated with energy metabolism processes in normal and pathological cells. In the present study, we evaluated the expression of MCT1, MCT2, and MCT4 and the contribution of these three MCT isoforms to L-lactate uptake in hepatocellular carcinoma (HCC) cells. In HepG2 and Huh-7 cells, L-lactate transport was pH-dependent, which is characteristic of MCT1, MCT2, and MCT4. Furthermore, L-lactate uptake was selectively inhibited by MCT1 and MCT4 inhibitors in HepG2 and Huh-7 cells. Kinetic analysis of HepG2 cells demonstrated that L-lactate uptake was biphasic. Although the knockdown of MCT1 and MCT4 in the HepG2 cells decreased the uptake of L-lactate, the knockdown of MCT2 had no effect on the uptake of L-lactate. Consequently, we concluded that both MCT1 and

MCT4 were involved in the transport of L-lactate in HepG2 and Huh-7 cells at pH 6.0. In contrast, PXB-cells，freshly isolated hepatocytes from humanized mouse livers, showed lower MCT4 expression and L-lactate uptake at pH 6.0 compared to that in HCC cell lines. In conclusion, MCT4, which contributes to L-lactate transport in HCC cells, is significantly different in HCC compared to normal hepatocytes, and has potential as a target for HCC treatment.

Keywords: L-lactate; transport; monocarboxylate transporter; HepG2 cell; PXB-cells

Abbreviations: CHC, α-cyano-4-hydroxycinnamate; HCC, hepatocellular carcinoma; MCT, monocarboxylate transporter; OXPHOS, oxidative phosphorylation; GAPDH, glyceraldehyde-3-phosphate dehydrogenase

Introduction

Monocarboxylate transporters (MCTs) are members of the solute carrier 16 (SLC16) family, and there are 14 isoforms of MCTs (Halestrap & Wilson, 2012). Four MCT isoforms, MCT1, MCT2, MCT3, and MCT4, which are encoded by *SLC16A1*, *SLC16A7*, *SLC16A8*, and *SLC16A3*, respectively, transport monocarboxylate compounds, such as L-lactate and pyruvate, which are energy metabolites of oxidative phosphorylation (OXPHOS) and glycolysis, with protons (H^+) (Halestrap, 2013). Thus, MCT1–4 contribute to the maintenance of energy balance and intracellular pH. Excluding MCT3, which is localized in the retina, MCT1, MCT2, and MCT4 are expressed in various tissues of the human body and have different areas of localization and functions (Fisel et al., 2018). MCT1 can bidirectionally import and export substrates and is ubiquitously expressed in human tissues. MCT2 is a high-affinity transporter involved in OXPHOS and gluconeogenesis and is expressed in the neurons, heart, liver, kidney, and testis. MCT4 is expressed in the brain, liver, small intestine, leukocytes, and white muscle fibers. MCT4 is a low-affinity transporter that is mainly responsible for exporting substrates. Furthermore, the expression and roles of MCT1 and MCT4 have been reported in not only normal cells but also pathological cells (Payen et al., 2020). While normal human cells mainly earn intracellular energy from OXPHOS in the mitochondria,

cancer cells generally derive their energy supply from glycolysis, which converts glucose into pyruvate and then L-lactate without the requirement of oxygen. Hence, MCT1 and MCT4 are expressed at high levels and contribute to the influx and efflux of L-lactate in cancer cells. In addition, MCTs and L-lactate have been proposed to make the extracellular environment more acidic and to be involved in tumor development and progression (Contreras-Baeza et al., 2019). Therefore, evaluating the mechanism underlying the transport of L-lactate in normal and pathological cells is important for elucidating the roles of MCTs and L-lactate.

We have previously studied mechanisms underlying the transport and regulatory effects of MCT1, MCT2, and MCT4 to elucidate their physiological and pathological roles (Kobayashi et al., 2021; Yamaguchi et al., 2020). We also studied the differences in the expression and function of MCTs in different types of cells. Sasaki et al. (2016) revealed that the uptake of L-lactate is mediated solely by MCT4 in human colon adenocarcinoma (Caco-2) cells expressing the MCT1, MCT2, and MCT4 proteins. Ideno et al. (2018) reported that L-lactate uptake in NHA cells as a human astrocyte model is mediated by MCT1, even though both MCT1 and MCT4 are expressed in human astrocytes. By identifying the MCT isoforms that transport L-lactate, we can reveal the mechanism underlying energy consumption in different types of cells.

Although Jeon et al. (2018) reported that MCT1, MCT2, and MCT4 are expressed in human hepatocellular carcinoma (HCC) cell lines, such as HepG2 and Huh-7, it is still unclear which transporter is involved in L-lactate transport. In the present study, we aimed to investigate the contribution of MCT1, MCT2, and MCT4 to L-lactate transport in HCC cell lines and compared their gene expression patterns as well as L-lactate uptake with that of PXB-cells, freshly isolated human hepatocytes from the liver of humanized chimeric mice (PXB-mice).

Materials and Methods

Chemicals

[^{14}C]-labeled L-lactic acid sodium salt (NEC599050UC) was purchased from PerkinElmer (Waltham, MA, USA). All of the other reagents used in this study were commercially available and of the highest possible purity.

Cell culture

The HepG2 cells (RIKEN BioResource Research Center, Ibaraki, Japan) and Huh-7 cells (JCRB Cell Bank, Osaka, Japan) were grown in Dulbecco's modified Eagle's medium (DMEM, Sigma-Aldrich, St. Louis, MO, USA) supplemented with 10% fetal bovine serum (FBS) and 1% penicillin- streptomycin (Sigma-Aldrich). In this study, the HepG2 cells between the 25th and 40th passages and the Huh-7 cells between the 85th and 95th passages were used. PXB-cells were seeded on 12-well and 24-well plates at PhoenixBio (Hiroshima, Japan). Yamasaki et al. (2020) showed that the expression of hepatic metabolic enzymes, such as cytochrome P450, and important transporters, such as organic anion transporting polypeptides, were stabilized approximately one week after isolation from PXB-mice. We purchased PXB-cells from PhoenixBio and used them six days after isolation from PXB-mice, four days after arrival at our laboratory.

PXB-cells were cultured according to the manufacturer's protocol, and grown in a differentiation hepatocyte clonal growth medium (dHCGM; PhoenixBio) consisting of DMEM culture medium containing 5 mM glucose, 10% FBS, 50 nM dexamethasone, 20 mM HEPES, 0.25 μg/mL insulin, 15 μg/mL L-proline, 5 μg/mL epidermal growth factor, 2% dimethyl sulfoxide, 0.1 mM L-ascorbic acid 2-phosphate, 44 mM $NaHCO_3$, and penicillin-streptomycin. All the cells were incubated at 37°C in a 5% CO_2 atmosphere.

Determination of mRNA expression

For the polymerase chain reaction (PCR) analysis, the total RNA was reverse-transcribed using ReverTra Ace (Toyobo, Osaka, Japan). Quantitative polymerase chain reaction (qPCR) was performed using the KAPA SYBR Fast qPCR kit (Kapa Biosystems, Wilmington, MA, USA) and the following primer sequences*:* *SLC16A1*, forward 5′-CCAGCTCTGACCATGATTGG-3′ and reverse 5′-GGCGCCAGAGTACAGAGGAAC-3′; *SLC16A7*, forward 5′-TCGTGGGTGCACCAAGATTTT-3′ and reverse 5′-AATCCACCAATTTACCTGCAA-3′; *SLC16A3*, forward 5′-GTTGGGTTTGGCACTCAACTTCC-3′ and reverse 5′-CAGGAAGACAGGGCTACCTGCTG-3′; *glyceraldehyde-3-phosphate*

dehydrogenase (GAPDH), forward 5′-CAATGACCCCTTCATTGACC-3′ and reverse 5′-GACAAGCTTCCCGTTCTCAG-3′. The qPCR thermocycling protocol was: 40 cycles of denaturation at 95°C for 10 s; annealing at 57°C for 20 s; and extension at 72°C for 1 s. The PCR products were normalized to amplified *GAPDH*, which was the internal reference.

Western blotting

The cells were lysed in a lysis buffer supplemented with 60 mM tris-HCl (pH 6.8), 1% sodium dodecyl sulfate (SDS) and 1% protease inhibitor cocktail in distilled water. The lysate was kept on ice for 5 min and sonicated briefly at 4 °C. Then, the sample was centrifuged at 12,000 × g for 15 min at 4 °C, and the clear supernatant was collected. The protein concentration was determined using a Pierce® bicinchoninic acid (BCA) protein assay kit (Thermo Fisher Scientific, Waltham, MA, USA). All of the lysates were added to a loading buffer containing 0.1 M tris-hydrochloride, 4% SDS, 10% 2-mercaptoethanol, 20% glycerol, and 0.004% bromophenol blue. Proteins (10 μg) were subjected to SDS-polyacrylamide gel electrophoresis (SDS-PAGE) and electrophoretically transferred onto polyvinylidene difluoride membranes (Bio-Rad, Hercules, CA, USA). The membranes were blocked with PBS containing 0.05% Tween

20 (PBS/T) and 1% non-fat dry milk for 1 h at room temperature. After being washed with PBS/T, the membranes were incubated with the primary antibodies against MCT1 (1:200, SC-365501, Santa Cruz Biotechnology, Dallas, TX, USA), MCT2 (1:1,000, ab198272, Abcam, Cambridge, UK), MCT4 (1:1,000, 22787-1-AP, Proteintech Group, Rosemont, IL, USA), and actin (1:1,000, ab179467, Abcam) overnight at 4 °C. We used these primary antibodies after confirming their specificity for the target gene in target-expressing oocytes. The bands were detected using horseradish peroxidase (HRP)-conjugated secondary antibodies (1:4,000) and visualized using ECL™ Western Blotting Detection Reagents (Cytiva, Tokyo, Japan).

[^{14}C]L-lactate uptake

To provide the driving forces of MCT, We evaluated the uptake of L-lactate in HCC cells at pH 6.0. Three days before the uptake experiment, HepG2 and Huh-7 cells were seeded in 24-well collagen-coated plastic culture plates. After the culture medium was removed, the cells were washed with the transport buffer (0.5 mL). The buffer consisted of 140 mM NaCl, 3 mM KCl, 1 mM $CaCl_2$, 1 mM $MgCl_2$, and 5 mM glucose. The Na^+-free transport buffer was prepared by replacing the sodium component with N-methyl-D-glucamine. HEPES (pH 7.4–7.0) and MES (pH 6.5–5.5) were used as

buffers. The cells were incubated at 37 °C with the transport buffer containing 0.1 μCi/mL [^{14}C]L-lactate at pH 6.0. After the incubation, the cells were quickly washed with ice-cold buffer twice and solubilized in 0.2 N NaOH/1% SDS. To measure the radioactivity of the [^{14}C]L-lactate taken up by the cells, the samples were mixed with a 3 mL scintillation cocktail. The cellular protein concentration was determined using the BCA assay to normalize the radioactivity.

MCT knockdown by small interfering RNA (siRNA)

The siRNA transfection was optimized using Lipofectamine RNAiMAX (Thermo Fisher Scientific). Stealth siRNA against MCT1 (HSS185929), the negative control siRNA against MCT1 (Stealth RNAi Negative Control Medium GC Duplex), Silencer Select siRNA against MCT4 (s17416), and the negative control siRNA against MCT4 (Silencer Negative Control No. 1 siRNA) were purchased from Thermo Fisher Scientific. FlexiTube siRNA for MCT2 (SI04191348) and the negative control siRNA against MCT2 (AllStars Negative Control siRNA FlexiTube siRNA, SI03650318) were obtained from QIAGEN (Hilden, Germany). HepG2 cells were transfected with siRNA via reverse transfection at a final concentration of 10 nM. After the siRNA transfection

(24 h) was complete, the siRNA-transfected cells were used for various experiments after 48 h.

MTT assay

HepG2 and Huh-7 cells were seeded at a density of 10,000 cells/well and 5,000 cells/well on a 96-well plate. After 24 h, the cells were treated with MCT inhibitors (containing 0.5% dimethyl sulfoxide (DMSO)) for 48h. Cell viability was evaluated using the 3-(4,5-dimethylthiazol-2-yl)-2,5-diphenyl-tetrazolium bromide (MTT) in according with the manufacturer's instruction. The absorbance of the resulting reaction solution was measured using a test wavelength at 590 nm for the samples and a reference wavelength at 690 nm.

Statistical analysis

Statistical analyses of the data were performed using an unpaired Student's t-test or Dunnett's test. The data were analyzed using SigmaPlot 14.5, and differences were considered statistically significant at $p < 0.05$.

The following equation was used to establish the rate of cellular uptake of L-lactate:

$$V = (Vmax_1 [S])/(Km_1+[S]) + (Vmax_2 [S])/(Km_2+[S]) + Kd [S]$$

V is the rate of uptake of L-lactate, Vmax is the maximum rate of uptake of L-lactate, [S] is the concentration of L-lactate in the transport buffer, Km is the Michaelis–Menten constant, and Kd is the coefficient of passive diffusion.

Results

Involvement of MCTs in L-lactate uptake in HCC cell lines

First, we investigated the time course of L-lactate uptake in the HepG2 and Huh-7 cells at pH 6.0. The uptake of L-lactate at pH 6.0 was linear until 3 min in the HepG2 cells and 1 min in the Huh-7 cells (data not shown). Therefore, in the following experiments, we conducted the uptake study for 3 min in the HepG2 cells and 1 min in the Huh-7 cells. Next, we evaluated the effect of acidic conditions on the L-lactate uptake in HepG2 and Huh-7 cells. Consequently, the uptake of L-lactate was significantly increased when the extracellular condition was acidified (Figure 1a and S1a). To provide driving forces for MCTs, in the following experiments, we conducted the uptake study at pH 6.0. While MCTs are driven by H^+, sodium-dependent monocarboxylate transporters (SMCTs) are Na^+ co-transport carriers. Therefore, we also investigated the uptake of L-lactate in a sodium-free condition, the results of which demonstrated that a sodium-free condition had no effect on the uptake of L-lactate in HepG2 and Huh-7 cells (Figure 1b and S1b). In addition, we demonstrated MCT1, MCT2, and MCT4 mRNA level (Figure 2a) and protein expression (Figure 2b) in the HepG2 and Huh-7 cells. These results suggested that the transport of L-lactate in the HepG2 and Huh-7 cell lines were facilitated by any of these MCT isoforms.

Inhibition experiments for L-lactate uptake in HCC cell lines

To estimate MCT isoform(s) which contribute to L-lactate uptake in the HCC cell lines, we assessed the inhibitory effect on L-lactate uptake by using α-cyano-4-hydroxycinnamate (CHC), AZD3965, D-lactate (Figure 3a and S1c). The CHC, which is MCT1, MCT2, and MCT4 inhibitor, was found to significantly inhibit L-lactate uptake. We could confirm that AZD3965, a selective non-competitive inhibitor of MCT1 and MCT2, inhibited significantly the uptake of L-lactate in HepG2 cells and inhibited slightly in Huh-7 cells. D-lactate, which has an effect on MCT1 but not MCT4, was also observed to have an inhibitory effect on the uptake of L-lactate in the HCC cell lines. We further verified the contribution of MCT4 to L-lactate uptake using selective MCT4 inhibitors (Figure 3b and S1d). The fenofibrate anion has been reported to have a higher inhibitory effect on MCT4 than that on MCT1 (Wu et al., 2021). Moreover, we reported that bindarit, which has a similar structure to the fenofibrate anion, selectively and strongly inhibits MCT4 activity (Futagi et al., 2018). In this study, we used the fenofibrate anion and bindarit as selective MCT4 inhibitors, which significantly inhibited the uptake of L-lactate in HepG2 and Huh-7 cells.

Kinetic analyses of L-lactate uptake in the HepG2 cells

Inhibition experiments in two HCC cell lines show similar results for L-lactate transport, so we further verify the characteristics of L-lactate uptake in the HepG2 cells. To calculate the kinetic parameters for the uptake of L-lactate, we conducted L-lactate concentration-dependent uptake study in HepG2 cells. Figure 3c shows the saturability of the Michaelis–Menten type. The Eadie–Hofstee plots that were constructed indicated that L-lactate uptake was biphasic in HepG2 cells (Figure 3d). The parameter approximations calculated by the Eadie–Hofstee plots were as follows: low affinity, Km_1 and $Vmax_1$ were estimated to be 2.3 mM and 22 nmol/mg protein/min, respectively; high affinity, Km_2 and $Vmax_2$ were estimated to be 0.21 mM and 5.8 nmol/mg protein/min, respectively.

Effects of MCT knockdown on L-lactate uptake in the HepG2 cells

To evaluate the contribution of these MCT isoforms in the uptake of L-lactate, we used siRNA to knockdown the MCT isoforms in the HepG2 cells. While the MCT1, MCT2, and MCT4 siRNA led to decreased protein levels of MCT1, MCT2, and MCT4 (Figure 4a, c, e), each siRNA had no effect on the protein expression of the non-targeted MCT isoforms (Figure S2). Under MCT1 or MCT4 knockdown conditions, the uptake of

L-lactate was significantly reduced from the treatment with negative control (Figure 4b, f). In contrast, MCT2 knockdown had no effect on the uptake of L-lactate (Figure 4d).

Comparison of MCT expression and L-lactate uptake between the two HCC cell lines and PXB-cells

Recently, fresh human hepatocytes isolated from humanized chimeric mice livers, called PXB-cells, have been used as normal human hepatocytes in many pharmaceutical studies, including those investigating drug metabolism and expression of drug transporters (Harada et al., 2021; Hata et al., 2020; Yamasaki et al., 2020). In the present study, we showed that MCT1 and MCT4 contribute to L-lactate transport in HepG2 and Huh-7 cells. Hence, we further evaluated MCT1 and MCT4 protein expression in PXB-cells and compared it with their expression in HepG2 and Huh-7 cells (Figure 5a). While the MCT1 protein expression level was not significantly different, MCT4 protein expression in PXB-cells was lower than that in the two HCC cell lines. Moreover, the uptake of L-lactate at pH 6.0 for 1 min was higher in HepG2 and Huh-7 cells than that in PXB-cells (Figure 5b). Compared with normal hepatocytes, MCT4 is expressed at higher levels in HepG2 and Huh-7 cells; therefore, MCT4 may increase L-lactate uptake in these HCC cell lines.

Discussion

In the present study, we examined L-lactate transport by performing inhibition experiments in HepG2 and Huh-7 cell lines expressing MCT1, MCT2, and MCT4. Unlike the early-discovered MCT inhibitors, such as α-cyano-4-hydroxycinnamate (CHC), more potent MCT1 inhibitors, such as AZD3965, BAY-8002, and 7ACC2, have been recently reported (Wang et al., 2021). Among them, AZD3965, which selectively inhibits both MCT1 (Ki = 2 nM) and MCT2 (Ki = 20 nM) but not MCT4, reached the clinical stage and has been analyzing in clinical trials (Puri & Juvale, 2020). In the present study, AZD3965 significantly inhibited the transport of L-lactate. Futagi et al. (2018) reported that D-lactate (10 mM) inhibits L-lactate transport by MCT1 but not by MCT4 in *Xenopus laevis (X. laevis)* oocytes. We used D-lactate as the selective inhibitor of MCT1, and this significantly decreased the uptake of L-lactate in the HepG2 and Huh-7 cells. These results from the inhibition experiments suggest that MCT1 contributes to the uptake of L-lactate uptake in these HCC cell lines at pH 6.0. Although selective inhibitors of MCT1 have been discovered, there are few reports of selective inhibitors of MCT4. Futagi et al. (2018) reported that bindarit has high selectivity for MCT4 inhibition (Ki = 30 μM). In this study, we demonstrated that bindarit significantly inhibited L-lactate transport in HepG2 and Huh-7 cells. Likewise, the fenofibrate anion, which inhibits

MCT4 with a higher efficiency compared with its inhibition of MCT1，had an inhibitory effect on the uptake of L-lactate in these two HCC cell lines. We therefore suggest that MCT4 is involved in the transport of L-lactate in HepG2 and Huh-7 cells at pH 6.0, in addition to MCT1.

In previous reports, we revealed that MCT1, MCT2, and MCT4 each have various levels of affinity for L-lactate at pH 5.5 in *X. laevis* oocytes; among these MCT isoforms, MCT2 has the lowest Km value for L-lactate (0.32 ± 0.02 mM), and the Km value of MCT1 (0.44 ± 0.03 to 1.0 ± 0.1 mM) is lower than that of MCT4 (2.8 ± 0.1 to 3.4 ± 0.4 mM) (Futagi et al., 2017; Sasaki et al., 2013, 2016; Yamaguchi et al., 2020). In the present study, the uptake of L-lactate at pH 6.0 in HepG2 cells was concentration-dependent and biphasic, and we calculated two Km values (0.21 and 2.3 mM) using the Eadie–Hofstee plot. These Km values were close to the Km values of MCT1, MCT2, and MCT4 for L-lactate, which were calculated in our previous reports. We considered that some transporters but not one of MCT1, MCT2 and MCT4 contribute to L-lactate uptake in the HepG2 cells. Furthermore, L-lactate uptake was significantly decreased by *SLC16A1* and *SLC16A3* knockdown but not by *SLC16A7* knockdown in HepG2 cells. In addition to the above inhibitory experiments, the kinetic analyses and

gene knockdown experiments supported the conclusion that MCT1 and MCT4 contribute to the uptake of L-lactate in HepG2 and Huh-7 cells at pH 6.0.

MCT2 protein was detected in HepG2 and Huh-7 cell lines by western blotting, but *SLC16A7* mRNA was not. Some studies have suggested that MCT2 is regulated at the translational level (Chiry et al., 2008; Zhang et al., 2007). They also suggested that MCT2 protein has been shown to be highly expressed even if its mRNA abundance is low in neurons. In this study, we similarly observed that *SLC16A7* mRNA levels did not correlate with its protein levels in HCC cell lines. In contrast, although MCT2 protein was found in these HCC cell lines, we revealed that the MCT2 contribution to L-lactate uptake is small under the present experimental condition. MCT2 has a higher affinity for pyruvate than for L-lactate (Halestrap, 2013). Moreover, McClelland et al. (2003) and Valença et al. (2015) reported that MCT2 localizes to the cellular membrane and peroxisomes. Accordingly, in HepG2 and Huh-7 cells, MCT2 may transport other substrates, such as pyruvate, or have intracellular functions other than L-lactate transport.

Some clinical studies have suggested that MCT4 is associated with HCC pathology. Alves et al. (2014) reported that the MCT4 level in the plasma membrane of primary HCC cells tends to be higher than that in non-neoplastic cells. Additionally, increased MCT4 expression has been reported to correlate with early recurrence and poor

prognosis in patients with HCC (Chen et al., 2018). In this study, we revealed that MCT4 protein expression in HepG2 and Huh-7 cancer cells was much higher than that in PXB-cells, that is, normal human hepatocytes. In other words, MCT4 expression in normal hepatocytes was lower than that in HCC cells, consistent with previous clinical studies. Therefore, we suggest that PXB-cells are suitable as normal hepatocytes for comparison with HCC cells when validating the therapeutic benefits of selectively inhibiting MCT4.

Additionally, the uptake of L-lactate at pH 6.0 was also higher in HepG2 and Huh-7 cells than that in PXB-cells. We conducted an uptake study at pH 6.0 in the present study to evaluate the activity of MCTs. The normal pH in the human body is approximately 7.4. The tumor microenvironment presents a low-pH environment (Boedtkjer & Pedersen, 2020). MCT4 is highly expressed in HCC tissues and plays an important role in transporting L-lactate in a low-pH environment. In the present study, we suggested that MCT4 selective inhibitors such as bindarit (500 μM) and fenofibrate anion (500 μM) suppressed HepG2 and Huh-7 cell growth (Figure S3a, b). In addition, we showed that the knockdown of MCT4 also suppressed these HCC cells growth (Figure S3c). Zhao et al. (2019) reported that targeted inhibition of MCT4 by microRNAs suppressed HCC growth *in vivo*. MCT4 selective inhibitors may suppress HCC cell

growth without affecting the viability of normal hepatocytes. Further studies on MCT4 selective inhibitors may lead to the development of new anticancer drugs that have low effects on normal hepatocytes.

Conclusion

We found that MCT1 and MCT4, but not MCT2, contributed to the uptake of L-lactate at pH 6.0 in HepG2 and Huh-7 cell lines. To our knowledge, this is the first study to evaluate the contribution of MCTs in L-lactate transport in HCC cell lines. Additionally, we observed higher MCT4 expression in these cell lines than that in PXB cells. Therefore, we discovered that high MCT4 expression in HCC cells contributes to L-lactate transport and has the potential to serve as a novel target for HCC treatment.

Acknowledgements

This work was supported by the Japan Society for the Promotion of Science KAKENHI (grant number 20K07171) (provided to M.K.). We would like to thank Editage (www.editage.com) for the English language editing.

Declaration of conflicts of interest statement

No potential conflicts of interest were reported by the authors.

References

Alves, V. A., Pinheiro, C., Morais-Santos, F., Felipe-Silva, A., Longatto-Filho, A., & Baltazar, F. (2014). Characterization of monocarboxylate transporter activity in hepatocellular carcinoma. *World Journal of Gastroenterology*, *20*(33), 11780–11787. https://doi.org/10.3748/wjg.v20.i33.11780

Boedtkjer, E., & Pedersen, S. F. (2020). The Acidic Tumor Microenvironment as a Driver of Cancer. *Annual Review of Physiology*, *82*, 103–126. https://doi.org/10.1146/annurev-physiol-021119-034627

Chen, H. L., OuYang, H. Y., Le, Y., Jiang, P., Tang, H., Yu, Z. S., He, M. K., Tang, Y. Q., & Shi, M. (2018). Aberrant MCT4 and GLUT1 expression is correlated with early recurrence and poor prognosis of hepatocellular carcinoma after hepatectomy. *Cancer Medicine*, *7*(11), 5339–5350. https://doi.org/10.1002/cam4.1521

Chiry, O., Fishbein, W. N., Merezhinskaya, N., Clarke, S., Galuske, R., Magistretti, P. J., & Pellerin, L. (2008). Distribution of the monocarboxylate transporter MCT2 in human cerebral cortex: An immunohistochemical study. *Brain Research*, *1226*, 61–69. https://doi.org/10.1016/j.brainres.2008.06.025

Contreras-Baeza, Y., Sandoval, P. Y., Alarcón, R., Galaz, A., Cortés-Molina, F., Alegriá, K., Baeza-Lehnert, F., Arce-Molina, R., Guequén, A., Flores, C. A., Martín, A. S.,

& Barros, L. F. (2019). Monocarboxylate transporter 4 (MCT4) is a high affinity transporter capable of exporting lactate in high-lactate microenvironments. *Journal of Biological Chemistry*, *294*(52), 20135–20147. https://doi.org/10.1074/jbc.RA119.009093

Fisel, P., Schaeffeler, E., & Schwab, M. (2018). Clinical and Functional Relevance of the Monocarboxylate Transporter Family in Disease Pathophysiology and Drug Therapy. *Clinical and Translational Science*, *11*(4), 352–364. https://doi.org/10.1111/cts.12551

Futagi, Y., Kobayashi, M., Narumi, K., Furugen, A., & Iseki, K. (2018). Identification of a selective inhibitor of human monocarboxylate transporter 4. *Biochemical and Biophysical Research Communications*, *495*(1), 427–432. https://doi.org/10.1016/j.bbrc.2017.10.025

Futagi, Y., Sasaki, S., Kobayashi, M., Narumi, K., Furugen, A., & Iseki, K. (2017). The flexible cytoplasmic loop 3 contributes to the substrate affinity of human monocarboxylate transporters. *Biochimica et Biophysica Acta - Biomembranes*, *1859*(10), 1790–1795. https://doi.org/10.1016/j.bbamem.2017.05.014

Halestrap, A. P. (2013). The SLC16 gene family-Structure, role and regulation in health and disease. *Molecular Aspects of Medicine*, *34*(2–3), 337–349.

https://doi.org/10.1016/j.mam.2012.05.003

Halestrap, A. P., & Wilson, M. C. (2012). The monocarboxylate transporter family-Role and regulation. *IUBMB Life*, *64*(2), 109–119. https://doi.org/10.1002/iub.572

Harada, K., Kohara, H., Yukawa, T., Matsumiya, K., & Shinozawa, T. (2021). Cell-based high-throughput screening for the evaluation of reactive metabolite formation potential. *Toxicology in Vitro*, *74*, 105159. https://doi.org/10.1016/j.tiv.2021.105159

Hata, K., Tomatsu, S., Takahashi, M., Sasaki, A., Umekawa, Y., Miyashita, K., Ogura, K., Toshima, G., Maeda, M., Takahashi, J., & Kakuni, M. (2020). Lipoprotein profile and lipid metabolism of pxb-cells®, human primary hepatocytes from liver-humanized mice: proposal of novel in vitro system for screening anti-lipidemic drugs. *Biomedical Research (Japan)*, *41*(1), 33–42. https://doi.org/10.2220/biomedres.41.33

Ideno, M., Kobayashi, M., Sasaki, S., Futagi, Y., Narumi, K., Furugen, A., & Iseki, K. (2018). Involvement of monocarboxylate transporter 1 (SLC16A1) in the uptake of L-lactate in human astrocytes. *Life Sciences*, *192*, 110–114. https://doi.org/10.1016/j.lfs.2017.10.022

Jeon, J. Y., Lee, M., Whang, S. H., Kim, J.-W., Cho, A., & Yun, M. (2018). Regulation

of Acetate Utilization by Monocarboxylate Transporter 1 (MCT1) in Hepatocellular Carcinoma (HCC). *Oncology Research Featuring Preclinical and Clinical Cancer Therapeutics*, *26*(1), 71–81. https://doi.org/10.3727/096504017X14902648894463

Kobayashi, M., Narumi, K., Furugen, A., & Iseki, K. (2021). Transport function, regulation, and biology of human monocarboxylate transporter 1 (hMCT1) and 4 (hMCT4). In *Pharmacology and Therapeutics* (Vol. 226). Elsevier Inc. https://doi.org/10.1016/j.pharmthera.2021.107862

McClelland, G. B., Khanna, S., González, G. F., Butz, C. E., & Brooks, G. A. (2003). Peroxisomal membrane monocarboxylate transporters: Evidence for a redox shuttle system? *Biochemical and Biophysical Research Communications*, *304*(1), 130–135. https://doi.org/10.1016/S0006-291X(03)00550-3

Payen, V. L., Mina, E., Van Hée, V. F., Porporato, P. E., & Sonveaux, P. (2020). Monocarboxylate transporters in cancer. *Molecular Metabolism*, *33*(July 2019), 48–66. https://doi.org/10.1016/j.molmet.2019.07.006

Puri, S., & Juvale, K. (2020). Monocarboxylate transporter 1 and 4 inhibitors as potential therapeutics for treating solid tumours: A review with structure-activity relationship insights. *European Journal of Medicinal Chemistry*, *199*, 112393.

https://doi.org/10.1016/j.ejmech.2020.112393

Sasaki, S., Futagi, Y., Ideno, M., Kobayashi, M., Narumi, K., Furugen, A., & Iseki, K. (2016). Effect of diclofenac on SLC16A3/MCT4 by the Caco-2 cell line. *Drug Metabolism and Pharmacokinetics*, *31*(3), 218–223. https://doi.org/10.1016/j.dmpk.2016.03.004

Sasaki, S., Kobayashi, M., Futagi, Y., Ogura, J., Yamaguchi, H., Takahashi, N., & Iseki, K. (2013). Crucial Residue Involved in L-Lactate Recognition by Human Monocarboxylate Transporter 4 (hMCT4). *PLoS ONE*, *8*(7), 3–9. https://doi.org/10.1371/journal.pone.0067690

Valença, I., Pértega-Gomes, N., Vizcaino, J. R., Henrique, R. M., Lopes, C., Baltazar, F., & Ribeiro, D. (2015). Localization of MCT2 at peroxisomes is associated with malignant transformation in prostate cancer. *Journal of Cellular and Molecular Medicine*, *19*(4), 723–733. https://doi.org/10.1111/jcmm.12481

Wang, N., Jiang, X., Zhang, S., Zhu, A., Yuan, Y., Xu, H., Lei, J., & Yan, C. (2021). Structural basis of human monocarboxylate transporter 1 inhibition by anti-cancer drug candidates. *Cell*, *184*(2), 370-383.e13. https://doi.org/10.1016/j.cell.2020.11.043

Wu, P., Zhou, Y., Guo, Y., Zhang, S. L., & Tam, K. Y. (2021). Recent developments of

human monocarboxylate transporter (hMCT) inhibitors as anticancer agents. *Drug Discovery Today*, *26*(3), 836–844. https://doi.org/10.1016/j.drudis.2021.01.003

Yamaguchi, A., Narumi, K., Furugen, A., Iseki, K., & Kobayashi, M. (2020). Identification of the essential extracellular aspartic acids conserved in human monocarboxylate transporters 1, 2, and 4. *Biochemical and Biophysical Research Communications*, *529*(4), 1061–1065. https://doi.org/10.1016/j.bbrc.2020.06.068

Yamasaki, C., Ishida, Y., Yanagi, A., Yoshizane, Y., Kojima, Y., Ogawa, Y., Kageyama, Y., Iwasaki, Y., Ishida, S., Chayama, K., & Tateno, C. (2020). Culture density contributes to hepatic functions of fresh human hepatocytes isolated from chimeric mice with humanized livers: Novel, long-term, functional two-dimensional in vitro tool for developing new drugs. *PLoS ONE*, *15*(9 September), 1–24. https://doi.org/10.1371/journal.pone.0237809

Zhang, S. X. L., Searcy, T. R., Wu, Y., Gozal, D., & Wang, Y. (2007). Alternative promoter usage and alternative splicing contribute to mRNA heterogeneity of mouse monocarboxylate transporter 2. *Physiological Genomics*, *32*(1), 95–104. https://doi.org/10.1152/physiolgenomics.00192.2007

Zhao, Y., Li, W., Li, M., Hu, Y., Zhang, H., Song, G., Yang, L., Cai, K., & Luo, Z. (2019). Targeted inhibition of MCT4 disrupts intracellular pH homeostasis and

confers self-regulated apoptosis on hepatocellular carcinoma. *Experimental Cell Research*, *384*(1), 111591. https://doi.org/10.1016/j.yexcr.2019.111591

Figure captions

Figure 1: The pH-dependence and Na^+-dependence of L-lactate uptake in the HepG2 cells.

(a) Uptake of L-lactate (0.64 μM) in HepG2 cells was measured in transport buffer for 3 min at 37°C at five pH values in the range of pH 5.5 to 7.4. The data are presented as the mean ± standard error (SE) of three independent experiments. (b) The uptake of L-lactate (0.64 μM) in HepG2 cells was measured in the presence or absence of Na^+ for 3 min. The data are presented as the mean with SE of three independent experiments.

Figure 2: MCT1, MCT2, and MCT4 expression in HCC cell lines.

(a) The expression pattern of *SLC16A1* (MCT1), *SLC16A7* (MCT2), and *SLC16A3* (MCT4) in HepG2 (gray circle) and Huh-7 (white circle) cells was analyzed using qPCR. Each gene expression level was normalized to that of *GAPDH*. Calculated averages are shown as black bar symbols. Genes showing a cycle threshold (C_t) value of more than 35 were considered inaccurate and annotated as not detectable (ND). (b) Protein expression of MCT1 (40–48 kDa), MCT2 (52 kDa), MCT4 (42–45 kDa), and actin (42 kDa) in the HepG2 and Huh-7 cells was analyzed by western blot.

Figure 3: Inhibition experiments and concentration dependence for the uptake of L-lactate in the HepG2 cells.

(a) Uptake of L-lactate (0.64 μM) in the presence of CHC (1 mM), AZD3965 (1 μM), and D-lactate (10 mM) at pH 6.0 for 3 min. The data are presented as the percentage relative to the uptake in the absence of an inhibitor (control). *, $p < 0.05$ and **, $p < 0.01$ compared with the control using Dunnett's test. The data are presented as the mean with standard error (SE) of three independent experiments. (b) Uptake of L-lactate (0.64 μM) in the presence of the fenofibrate anion (100 μM) and bindarit (100 μM) at pH 6.0 for 3 min. The data are presented as the mean with SE of three to four independent experiments. The data are presented as the percentage relative to the uptake in the absence of an inhibitor (control). **, $p < 0.01$ compared with the control using Dunnett's test. (c) The uptake of L-lactate in HepG2 cells was measured in transport buffer (pH 6.0) for 3 min at 8 concentrations of L-lactate (in the range of 0.00064–10 mM). The data are presented as the mean ± SE of three independent experiments. (d) The Eadie–Hofstee plots of the L-lactate uptake data; V represents the uptake rate of L-lactate, and [S] represents the concentration of L-lactate in the buffer. The data are represented as the mean ± SE of three independent experiments.

Figure 4: Effects of MCT siRNA on MCT protein expression and uptake of L-lactate in the HepG2 cells.

(a) MCT1 and actin protein expression in HepG2 cells transfected with MCT1 siRNA. (b) Uptake of L-lactate in HepG2 cells transfected with MCT1 siRNA at pH 6.0 for 3 min. The data are presented as the percentage relative to the negative control. **, $p < 0.01$ compared with negative control using unpaired Student's t-test. The data are represented as the mean with standard error (SE) of three independent experiments. (c) MCT2 and actin protein expression in HepG2 cells transfected with MCT2 siRNA. (d) Uptake of L-lactate in HepG2 cells transfected with MCT2 siRNA at pH 6.0 for 3 min. The data are presented as the percentage relative to the negative control. The data are presented as the mean with SE of three independent experiments. (e) MCT4 and actin protein expression in HepG2 cells transfected with MCT4 siRNA. (f) Uptake of L-lactate in HepG2 cells transfected with MCT4 siRNA at pH 6.0 for 3 min. The data are presented as the percentage relative to the negative control. The data are presented as the mean with SE of three independent experiments. *, $p < 0.05$ compared with the negative control using unpaired Student's t-test.

Figure 5: The difference of MCT protein expression and the uptake of L-lactate transport between the HCC cell lines and PXB-cells.

(a) Protein expression of MCT1, MCT4, and actin in the HepG2, Huh-7 and PXB-cells was analyzed by western blot. (b) Uptake rate of L-lactate (0.64 μM) in three different cells was measured in transport buffer for 1 min at pH 6.0. The data are presented as the mean ± standard deviation (SD) of three determinations.

Supplemental Figure 1: The pH-dependence and Na^+-dependence of L-lactate uptake in the Huh-7 cells.

(a) Uptake of L-lactate (0.64 μM) in Huh-7 cells was measured in transport buffer for 1 min at five pH values in the range of pH 5.5 to 7.4 at 37°C. The data are presented as the mean ± standard deviation (SD) of three determinations. (b) The uptake of L-lactate in Huh-7 cells was measured in the presence or absence of Na^+ for 1 min. The data are presented as the mean with SD of three determinations. (c) Uptake of L-lactate (0.64 μM) in the presence of CHC (1 mM), AZD3965 (1 μM), and D-lactate (10 mM) at pH 6.0 for 1 min. The data are presented as the percentage relative to the uptake in the absence of an inhibitor (control). **, $p < 0.01$ compared with the control using Dunnett's test. The data are presented as the mean with standard error (SE) of three independent experiments. (d) Uptake of L-lactate (0.64 μM) in the presence of the fenofibrate anion (100 μM) and bindarit (100 μM) at pH 6.0 for 1 min. The data are presented as the mean with SE of

three independent experiments. The data are presented as the percentage relative to control. **, $p < 0.01$ compared with the control using Dunnett's test.

Supplemental Figure 2: Effects of MCT siRNA on MCT protein expression in the HepG2 cells.

MCT1, MCT2, MCT4, and actin protein expression in HepG2 cells transfected with MCT1, MCT2, and MCT4 siRNA. The final concentration of siRNA was 10 nM.

Supplemental Figure 3: The toxicity of MCT4 inhibitors and MCT4 knockdown by siRNA for HepG2 and Huh-7 cells.

3-(4,5-Dimethylthiazol-2-yl)-2,5-diphenyl tetrazolium bromide (MTT) assay of hepatocellular carcinoma HepG2 and Huh-7 cells (a) with 500 μM bindarit, (b) 500 μM fenofibrate anion, and (c) MCT4 knockdown by siRNA at 5 and 10 nM. *, $p < 0.05$ and **, $p < 0.01$ compared with the control or negative control, respectively, using Student's t-test. Data are presented as mean ± standard deviation (SD) of three determinations.

Figure 1

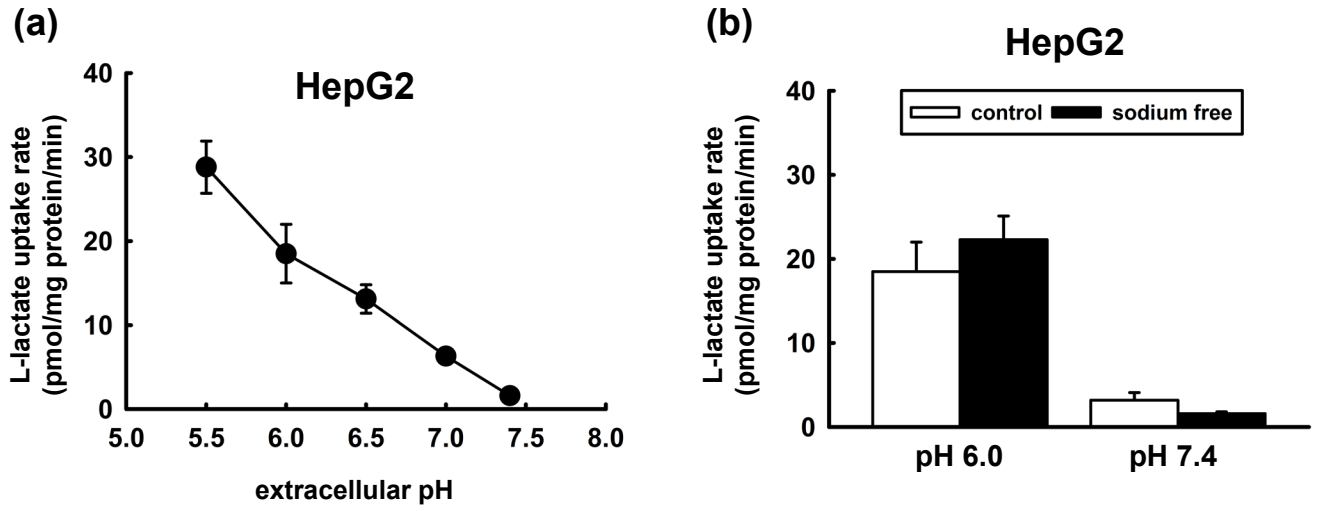

(a)
HepG2
L-lactate uptake rate (pmol/mg protein/min)
40
30
20
10
0
5.0
5.5
6.0
6.5
7.0
7.5
8.0
extracellular pH
(b)
HepG2
control
sodium free
L-lactate uptake rate (pmol/mg protein/min)
40
30
20
10
0
pH 6.0
pH 7.4

Figure 2

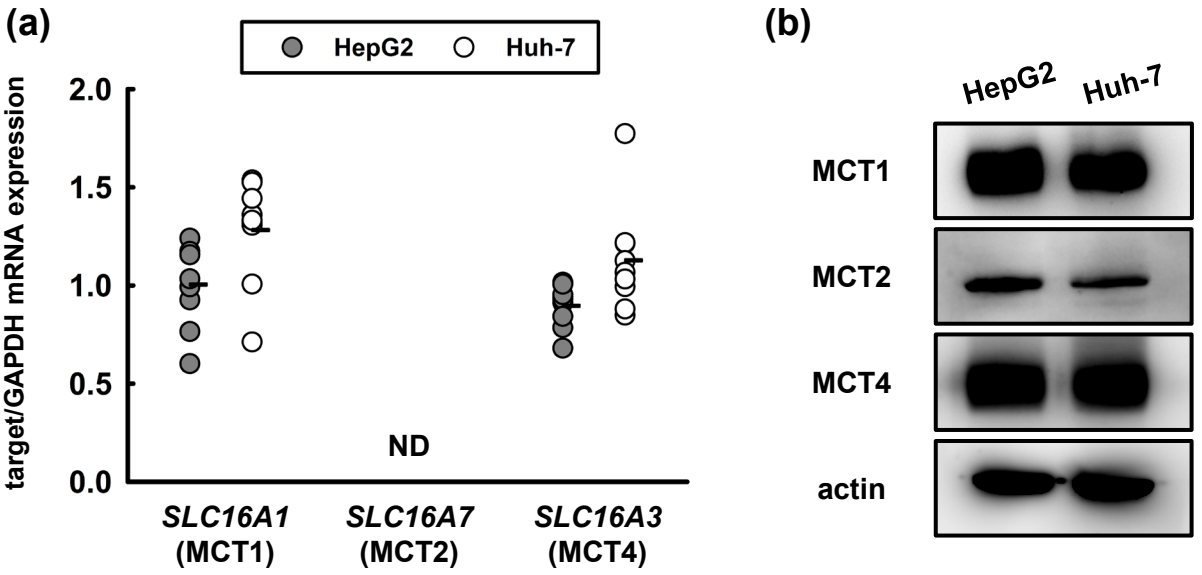

(a)
HepG2
Huh-7
target/GAPDH mRNA expression
2.0
1.5
1.0
0.5
0.0
ND
SLC16A1
(MCT1)
SLC16A7
(MCT2)
SLC16A3
(MCT4)
(b)
HepG2
Huh-7
MCT1
MCT2
MCT4
actin

Figure 3

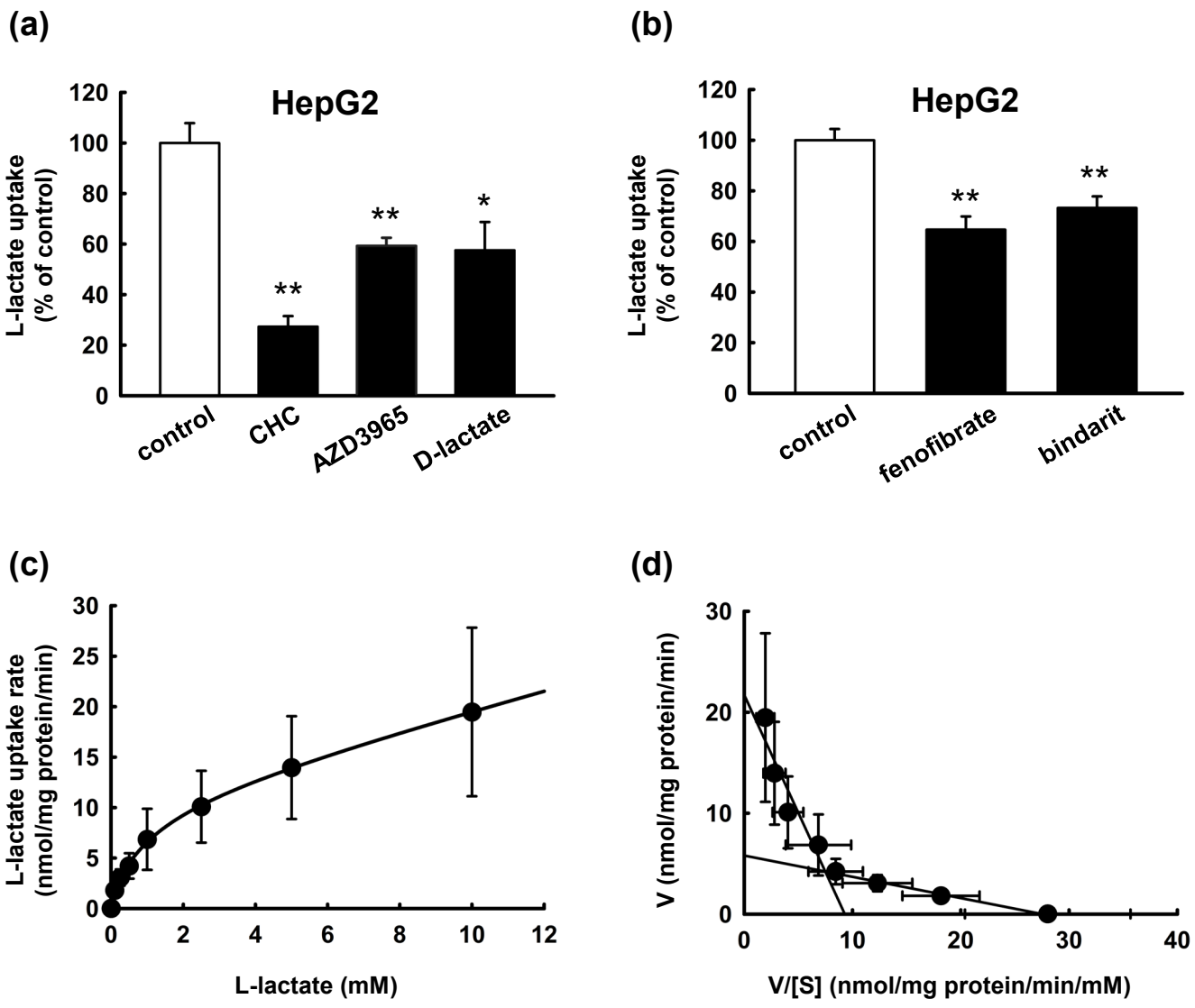

(a)
HepG2
L-lactate uptake (% of control)
120
100
80
60
40
20
0
**
**
*
control
CHC
AZD3965
D-lactate
(b)
HepG2
L-lactate uptake (% of control)
120
100
80
60
40
20
0
**
**
control
fenofibrate
bindarit
(c)
L-lactate uptake rate (nmol/mg protein/min)
30
25
20
15
10
5
0
0
2
4
6
8
10
12
L-lactate (mM)
(d)
V (nmol/mg protein/min)
30
20
10
0
0
10
20
30
40
V/[S] (nmol/mg protein/min/mM)

Figure 4

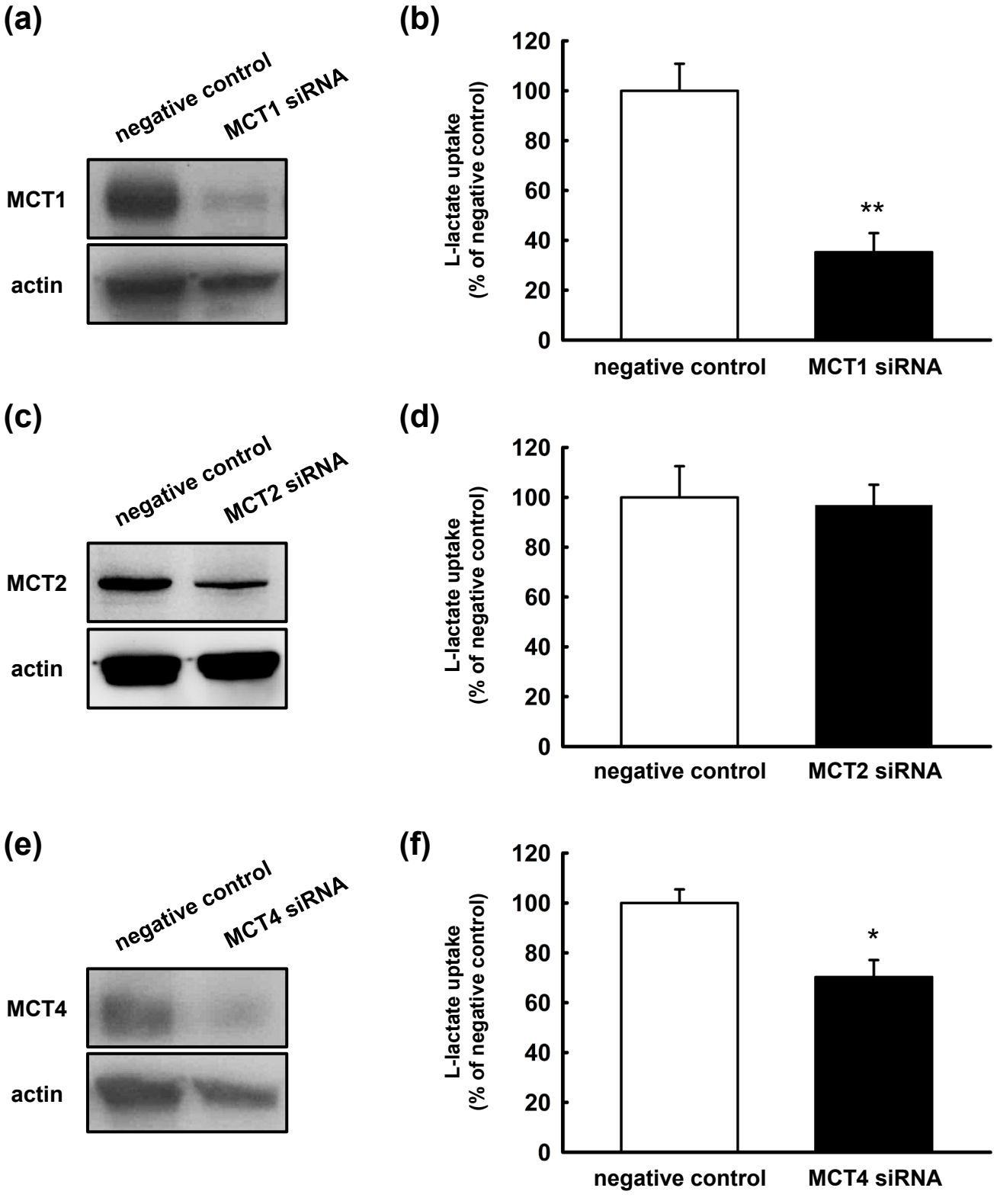
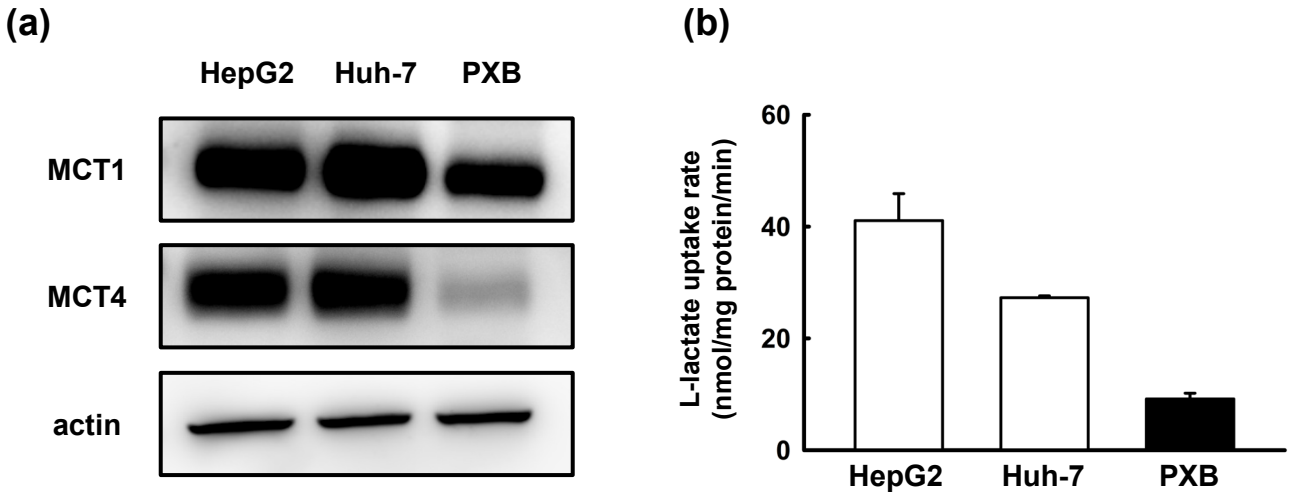
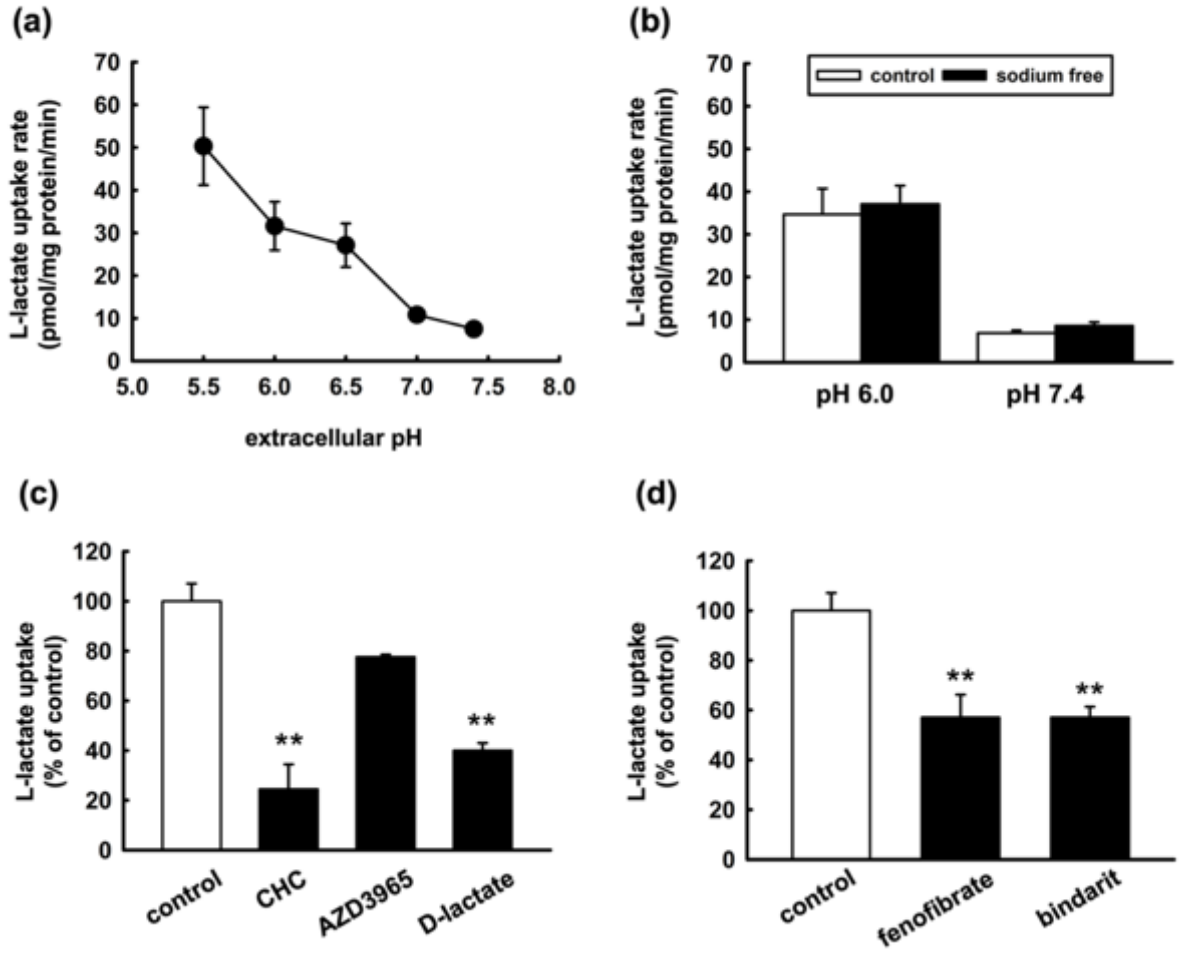

(a)
negative control
MCT1 siRNA
MCT1
actin
(b)
L-lactate uptake
(% of negative control)
120
100
80
60
40
20
0
**
negative control
MCT1 siRNA
(c)
negative control
MCT2 siRNA
MCT2
actin
(d)
L-lactate uptake
(% of negative control)
120
100
80
60
40
20
0
negative control
MCT2 siRNA
(e)
negative control
MCT4 siRNA
MCT4
actin
(f)
L-lactate uptake
(% of negative control)
120
100
80
60
40
20
0
*
negative control
MCT4 siRNA

Figure 5


(a)
HepG2
Huh-7
PXB
MCT1
MCT4
actin
(b)
L-lactate uptake rate
(nmol/mg protein/min)
60
40
20
0
HepG2
Huh-7
PXB

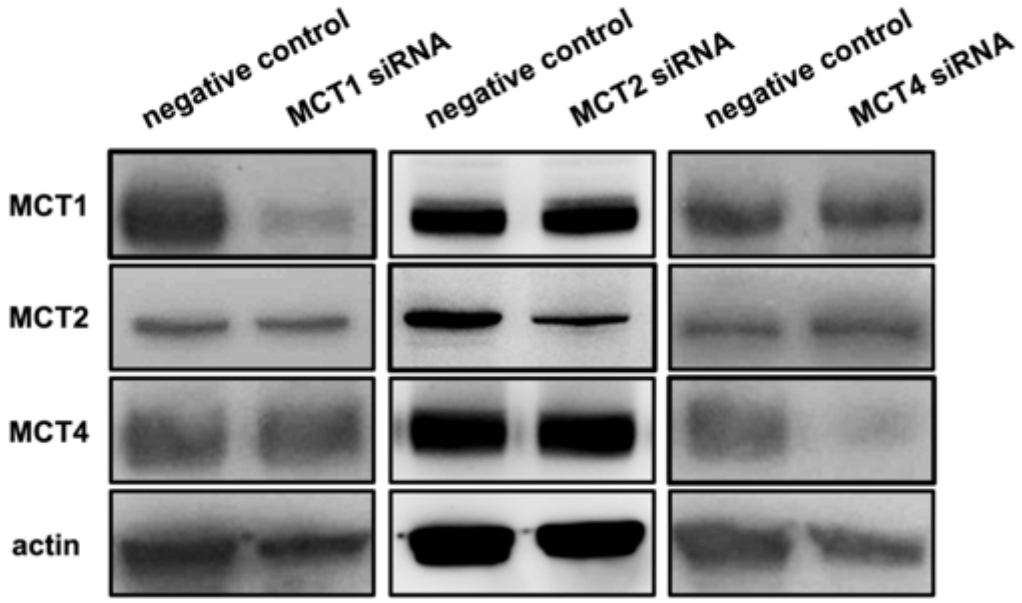
Supplemental Figure 1



Supplemental Figure 1: Involvement of MCTs in L-lactate uptake in the Huh-7 cells.

(a) Uptake of L-lactate (0.64 μM) in Huh-7 cells was measured in transport buffer for 1 min at five pH values in the range of pH 5.5 to 7.4 at 37°C. The data are presented as the mean ± standard deviation (SD) of three determinations. (b) The uptake of L-lactate in Huh-7 cells was measured in the presence or absence of Na^+ for 1 min. The data are presented as the mean with SD of three determinations. (c) Uptake of L-lactate (0.64 μM) in the presence of CHC (1 mM), AZD3965 (1 μM), and D-lactate (10 mM) at pH 6.0 for 1 min. The data are presented as the percentage relative to the uptake in the absence of an inhibitor (control). **, $p < 0.01$ compared with the control using Dunnett's test. The data are presented as the mean with standard error (SE) of three independent experiments. (d) Uptake of L-lactate (0.64 μM) in the presence of the fenofibrate anion (100 μM) and bindarit (100 μM) at pH 6.0 for 1 min. The data are presented as the mean with SE of three independent experiments. The data are presented as the percentage relative to control. **, $p < 0.01$ compared with the control using Dunnett's test.

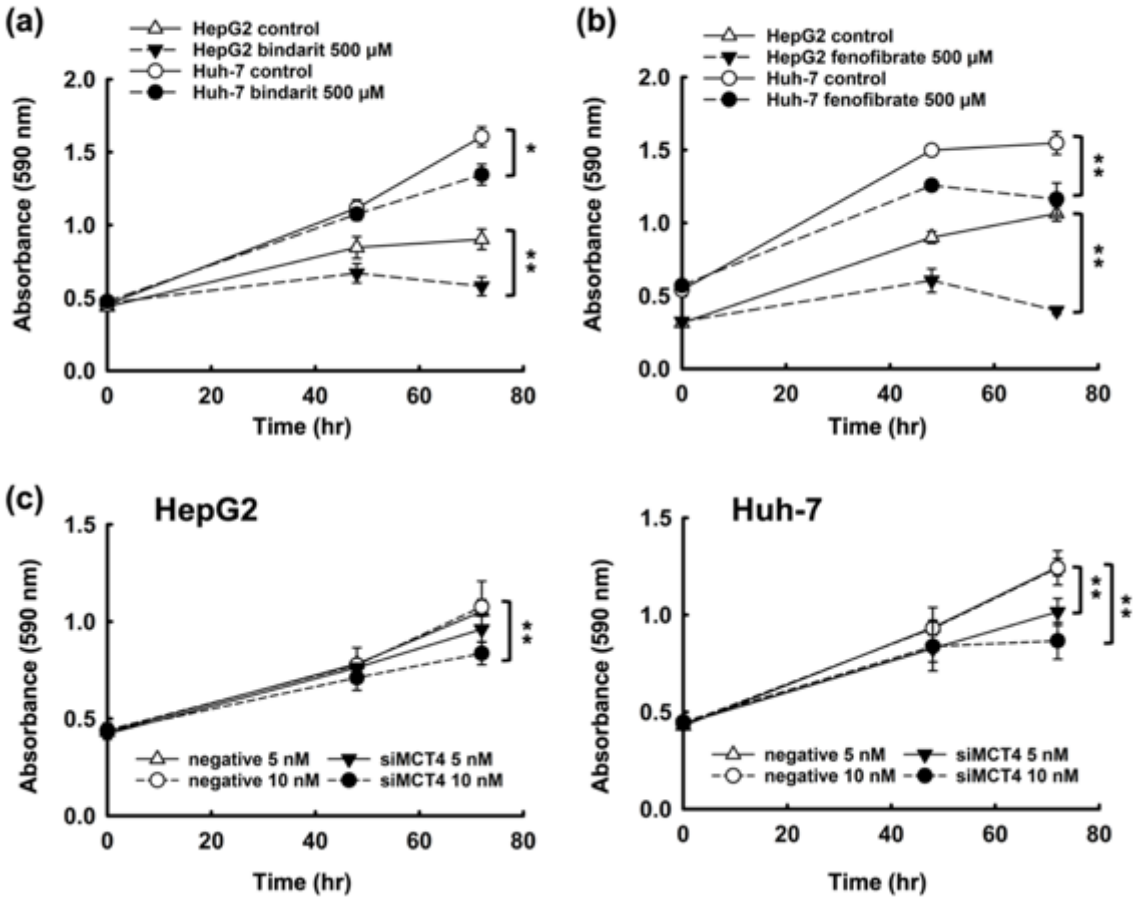
Supplemental Figure 2



Supplemental Figure 2: Effects of MCT siRNA on MCT protein expression in the HepG2 cells.

MCT1, MCT2, MCT4, and actin protein expression in HepG2 cells transfected with MCT1, MCT2, and MCT4 siRNA. The final concentration of siRNA was 10 nM.

Supplemental Figure 3



Supplemental Figure 3: The toxicity of MCT4 inhibitors and MCT4 knockdown by siRNA for HepG2 and Huh-7 cells.

3-(4,5-Dimethylthiazol-2-yl) 2,5-diphenyl tetrazolium bromide (MTT) assay of hepatocellular carcinoma HepG2 and Huh-7 cells (a) with 500 μM bindarit, (b) 500 μM fenofibrate anion, and (c) MCT4 knockdown by siRNA at 5 and 10 nM. *, $p < 0.05$ and **, $p < 0.01$ compared with the control or negative control, respectively, using Student's t-test. Data are presented as mean ± standard deviation (SD) of three determinations.